Journal of Materials Chemistry

Cite this: *J. Mater. Chem.*, 2011, **21**, 17505

www.rsc.org/materials

PAPER

Self-assembly of mesoporous TiO_2 nanospheres *via* aspartic acid templating pathway and its catalytic application for 5-hydroxymethyl-furfural synthesis†

Sudipta De,[a] Saikat Dutta,[a] Astam K. Patra,[b] Asim Bhaumik*[b] and Basudeb Saha*[a]

Received 11th July 2011, Accepted 1st September 2011
DOI: 10.1039/c1jm13229f

Self-assembled mesoporous TiO_2 nanoparticulate material with well-defined nanospherical morphologies was prepared by using DL-aspartic acid as a template. Powder XRD, TEM and SEM techniques were used to characterize the TiO_2 nanoparticles. The presence of high acid density in the mesoporous TiO_2 was confirmed by pyridine-IR and NH_3-TPD studies. This new mesoporous TiO_2 nanomaterial efficiently catalyzed the dehydration of D-fructose and D-glucose into 5-hydroxymethylfurfural in DMA-LiCl solvent under microwave assisted heating. The acidic sites of the TiO_2 nanomaterial were responsible for the dehydration reaction which produced a maximum 82.3% HMF.

Introduction

Titanium dioxide (TiO_2) has excellent chemicophysical properties and unique applications in several areas including photocatalysis, gas sensors, solar cells and Li-ion batteries.[1–5] Extensive research efforts have been focused on controlling the microstructure and morphology of TiO_2 to achieve novel and enhanced properties. Characteristically, mesoporous TiO_2 nanospheres have attracted great interest due to their high surface area, surface permeability, and light-trapping effect.[6–9] In recent years, TiO_2 material has been used extensively in environmental,[10] sensing,[11] photocatalytic,[12–14] and optoelectronic applications.[15,16] However, the major drawback of TiO_2 nanostructured materials for suitable applications is their low surface area and high band gap. The surface area of TiO_2 based materials can be enhanced significantly by introducing nanoscale porosity at its surface. The supramolecular assembly of ionic or neutral surfactants has been conventionally employed as a template or structure directing agent to design mesoporous materials.[17–19] TiO_2 material with mesoporosity can be prepared by templating with various agents such as dendrimers,[20] polymers,[21] aromatic acid.[22] Hierarchically anatase *meso*/nanoporous S- and C-doped TiO_2[23] and alcohothermal method derived TiO_2 microspheres[24] have been recently reported for their enhanced photocatalytic activity.

Amino acids, as typical biomolecules with polyfunctional groups, have a low softening point, selective adsorptivities and metal cation complexing ability. It was envisioned that amino acid could serve as a smart template in the preparation of nanoparticulate TiO_2 materials of desired structure based on their unique physical and chemical properties. A recent report on the fabrication of mesoporous TiO_2 with glycine templating inspired to explore other amino acids as templating agents to prepare TiO_2 nanoparticles of desired mesoporosity and Lewis acidity.[25] For this, TiO_2 materials have been prepared using various methods, including the soft-templating pathway, *e.g.* surfactant micelles as template[26,27] and also hard templating.[28] Generally, template method of preparation of titania nanoparticle involves calcinations at high temperatures to remove the template and leave behind pores in the TiO_2 matrix. During the calcination process, sintering and crystallization also occurs, which can cause collapse of the mesoporous structure, resulting in a significant loss in surface area. Thus, proper choice of the template molecule and its efficient removal from the surface TiO_2 matrix are highly desirable to achieve TiO_2 based nanostructured materials.

5-Hydroxymethylfurfural (HMF) is a biomass derived platform chemical for the synthesis of a range of value added compounds.[29,30] Several catalysts are known for the conversion of biomass and carbohydrates into HMF in ionic liquids, organic, aqueous, and aqueous-organic biphasic solvents.[31–33] Watanabe and co-workers have disclosed the effectiveness of anatase-TiO_2 material as catalyst for the conversion of fructose and glucose to HMF in hot compressed water (HCW) with 38.2% and 7.7% HMF yield at 200 °C.[34,35] NH_3- and CO_2-TPD (temperature programmed desorption) analysis revealed that anatase-TiO_2 material was acidic (acid density 17 μmol m^{-2} and base density 8.9 μmol m^{-2}). It was anticipated that the formation of HMF occurred from basic site driven isomerisation of glucose

[a]*Laboratory of Catalysis, Department of Chemistry, North Campus, University of Delhi, Delhi, 110007, India. E-mail: bsaha@chemistry.du.ac.in; Fax: +9127667794; Tel: +011-27666646*
[b]*Department of Materials Science, Indian Association for the Cultivation of Science, Jadavpur, Kolkata, 700032, India. E-mail: msab@iacs.res.in*

† Electronic supplementary information (ESI) available: ^1H and ^{13}C NMR data, HPLC spectra, and more results of experiments. See DOI: 10.1039/c1jm13229f

and acidic site driven dehydration of fructofuranose. Catalytic activity of the TiO_2 catalyst was also tested for the conversion of sugarcane bagasse, rice husk and corncob to HMF in HCW at 200 °C. The results showed that the yield of HMF was dependent on the catalyst preparation method and the acid density.[36]

Herein, we report the synthesis of self-assembly mesoporous TiO_2 nanoparticles from titanium isopropoxide in the presence of DL-aspartic acid as a template. The presence of high acidic sites inside the mesopores of the TiO_2 nanoparticles promoted the conversion of fructose and glucose into HMF.

Experimental

D-Glucose, D-fructose, 1-butyl-3-methylimidazolium chloride ([BMIM]Cl), DL-aspartic acid, titanium isopropoxide were supplied by Sigma-Aldrich and were used without further purification. Dimethylacetamide (DMA), dimethylsulfoxide (DMSO), lithium chloride, 25% ammonia solution were supplied by Spectrochem, India. Unless otherwise stated, distilled water was used as aqueous phase.

A JEOL JEM 6700F field emission scanning electron microscope (FESEM) was used for the determination of the particle morphology of the TiO_2 nanoparticles. HR-TEM images were recorded on a JEOL DATUM Model No. JEM1011. Fourier transform infrared (FTIR) spectra of the pyridine adsorbed samples were recorded on a Perkin Elmer Spectrum 100 spectrophotometer. For the temperature programmed desorption (TPD) of ammonia studies, sample was activated and then ammonia was injected at room temperature in the absence of carrier gas flow. The temperature was then raised in a stepwise manner at a linear heating rate of 10 °C min^{-1}. The desorbed ammonia in the temperature range of 100 to 750 °C was analyzed by using a Micromeritics ChemiSorb 2720 containing a thermal conductivity detector. Powder X-ray diffraction of the TiO_2 nanoparticles for wide-angle was carried out in a Rigaku Mini-Flex II XRD machine. Conversions of D-fructose and D-glucose into HMF were performed in a CEM Matthews WC Discover microwave reactor, model no. 908010 DV9068, equipped with programmable pressure and temperature controller. ^{1}H NMR spectral analysis was performed on a JEOL JNM ECX-400 P 400 MHz instrument and data were processed using a JEOL DELTA program version 4.3.6. The yield of HMF was determined by HPLC and UV-Visible spectrometric techniques. HPLC analysis of the reaction product was performed on a 20AD Shimadzu Instrument equipped with UV detector and pressure gradient pumps.

Preparation of TiO_2 from titanium isopropoxide and aspartic acid

2.662 g of DL-aspartic acid (20 mmol) was mixed with 15 mL of distilled water. The pH of the solution was maintained at pH = 7 by adding 20% sodium hydroxide solution to dissolve the aspartic acid. A titanium isopropoxide [$Ti(O^iPr)_4$] solution was prepared by adding 2.95 mL $Ti(O^iPr)_4$ (10 mmol) in 5 mL isopropyl alcohol. This solution was then slowly added into the aspartic acid solution. The pH of the mixed solution was then adjusted to pH = 10 by adding of ammonia solution (25%) and stirred for 2 h at room temperature. The resultant solid was collected by repeated centrifugation (8000 rpm, 10 min) and washing with distilled water. The material was dried in oven at 383 K for 8 h and then calcined at 773 K for 4 h.

Measurement of acid content of TiO_2 by temperature programmed desorption (TPD) analysis of ammonia

Temperature programmed desorption (TPD) analysis of ammonia was conducted by using Micromeritics ChemiSorb 2720 in the temperature range of 100 to 750 °C which employed a thermal conductivity detector. TiO_2 nanoparticles were activated at 300 °C inside the reactor of the TPD furnace under helium flow for 4 h. After cooling it to room temperature, ammonia was injected in the absence of carrier gas flow and the system was allowed to equilibrate. A current of helium was used to flush out the excess ammonia. The temperature was then raised in a programmable manner at a linear heating rate of 10 °C min^{-1}. The amounts of ammonia desorbed in the temperature values of 100–200, 200–400 and 400–750 °C were taken as measures of weak, medium and strong acid sites respectively.[37]

Procedure of conversion of glucose into HMF in DMSO

A microwave tube was charged with glucose (100 mg), TiO_2 catalyst (50 mg) and DMSO (2 g). The microwave tube, loaded with the reactants, was placed in the microwave reactor. The power of MW was set to 300 W. The reaction was allowed to continue for the desired time at pre-set temperature. After the reaction, the tube was cooled to room temperature and the reaction product was analyzed by HPLC and spectrophotometric techniques for measuring the HMF yield.

Procedure of conversion of glucose into HMF in DMA-LiCl

A microwave tube was charged with glucose (100 mg), TiO_2 catalyst (50 mg) and DMA-LiCl (2 g, 10 wt% LiCl). The microwave tube, loaded with the reactants, was placed in the microwave reactor. After the reaction, the reaction mixture was allowed to cool to room temperature and the reaction product was analyzed by HPLC and spectrophotometric techniques for measuring the HMF yield.

Catalyst life-time study in DMA-LiCl

A microwave tube was charged with fructose (100 mg), TiO_2 catalyst (50 mg) and DMA-LiCl (2 g, 10 wt% LiCl). The mixture was heated for 2 min under microwave irradiation at 140 °C. After the reaction, the reaction mixture was cooled down to room temperature and filtered. HMF component was extracted with diethyl ether. Spent TiO_2 catalyst was recovered, washed with distilled water and dried. The recovered catalyst was reused for five catalytic cycles.

Determination of HMF yield. The yield of HMF in the product solution was determined by HPLC and UV-Visible spectrophotometric techniques.

UV-Visible spectrophotometric method. The UV-Visible spectrum of pure HMF solution (Fig. S3†) has a distinct peak at

284 nm with corresponding extinction coefficient (ε) value of 1.66 × 10^4 $M^{-1}cm^{-1}$. The percentage of HMF in each of the reaction product as given in Table 1 was calculated from the measured absorbance values at 284 nm and the extinction coefficient value. Repeated measurement of the same solution showed the percentage of error associated with this measurement was ±3%.

HPLC method. HPLC measurements of the product solution were conducted using a LC 20AD Shimadzu Instrument equipped with a UV detector, pressure gradient pumps, C18 (250 × 4.6 mm × 5.0 micron) reverse phase column and temperature controller. The product solution was run through the HPLC column using 20 μL injection loop and 0.05% H_2SO_4 in water as a mobile phase at 35 °C. The flow rate of the mobile phase was set at 1.0 mL/min. The HMF peak was identified by its retention time in comparison with authentic sample and integrated. The actual concentration of HMF was determined from the pre-calibrated plot of peak area against concentrations.

Results and discussion

The wide angle XRD patterns of the TiO_2 nanoparticles (Fig. 1 (a)) suggested highly crystalline planes of anatase TiO_2. The crystalline planes corresponding to the peaks for anatase TiO_2 have been indexed in Fig. 1(a). The powder XRD results revealed that aspartic acid template method produced highly stable and crystalline TiO_2 nanoparticles.

The small angle XRD patterns of mesoporous TiO_2 is shown in Fig. 1(b). This figure shows one sharp peak corresponding to self-assembled nanoparticles with an average particle distribution length of *ca.* 10.6 nm. This self-assembled nanostructure is further revealed from the electron microscopic images. Representative TEM images of mesoporous TiO_2 nanoparticles calcined at 500 °C are shown in Fig. 1(c) and 1(d). As seen in these figures, spherical tiny TiO_2 nanoparticles of dimension 10–15 nm are assembled by forming self-aggregated (loose assembly) nanostructures. The selected area electron diffraction (SAED)

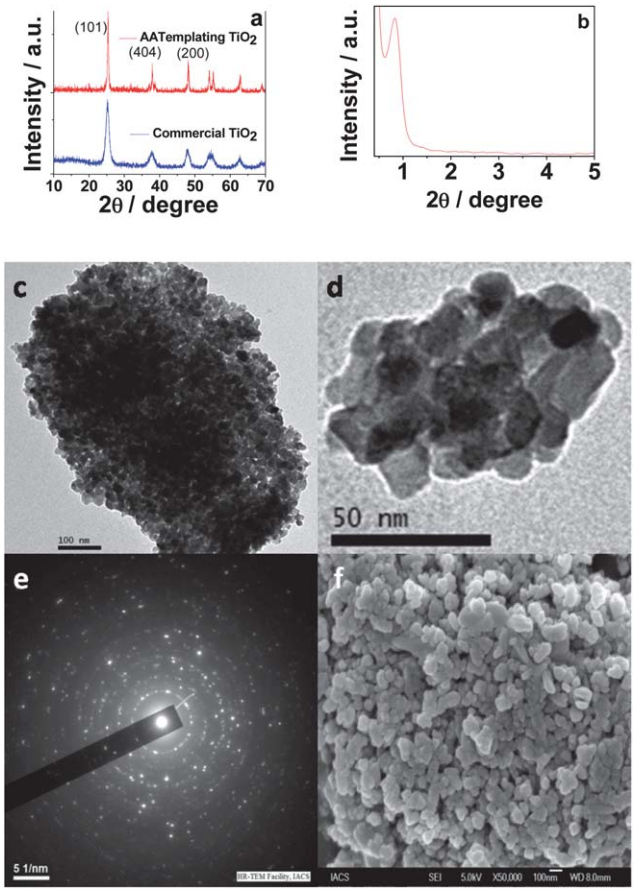

Fig. 1 **a**: Wide angle XRD profiles of the TiO_2 samples with indexed peaks compared with that of commercial anatase TiO_2 powder; **b**: Small angle XRD pattern of aspartic acid templated TiO_2 nanomaterial; **c**: TEM image of typical TiO_2 nanostructure; **d**: TEM image of calcined (500 °C) TiO_2 sample; **e**: Selected area electron diffraction (SAED) pattern of the calcined mesoporous TiO_2 sample; **f**: FESEM image of the self-assembled mesoporous TiO_2 nanoparticles.

Table 1 Results of microwave assisted conversion of fructose and glucose into HMF catalyzed by mesoporous TiO_2

Entry	Substrate (100 mg)	Solvent (2 g)	TiO_2 (mg)	Additive [BMIM]Cl, wt (%)	*T*/°C	*t*(min)	HMF yield (%)[a]	HMF yield (%)[b]
1	Fructose	Water	—	—	120	2	1.2	—
2	Fructose	Water	50	—	120	2	31.5	30.2
3	Fructose	DMSO	—	—	130	2	23.6	24.1
4	Fructose	DMSO	50	—	130	2	49.5	47.8
5	Fructose	DMA-LiCl (10%)	—	—	130	2	61.0	60.2
6	Fructose	DMA-LiCl (10%)	50	—	130	2	74.8	74.2
7	Fructose	DMA-LiCl (10%)	50	20	130	2	82.3	81.6
8	Glucose	Water	—	—	120	2	0	—
9	Glucose	Water	50	—	120	2	13.4	—
10	Glucose	Water	50	—	120	5	18.9	—
11	Glucose	DMSO	—	—	130	2	11.7	—
12	Glucose	DMSO	50	—	130	2	26.1	25.6
13	Glucose	DMA-LiCl (10%)	—	—	130	2	4.1	—
14	Glucose	DMA-LiCl (10%)	50	—	130	2	21.5	20.4
15	Glucose	DMA-LiCl (10%)	50	20	130	2	30.2	30.1

[a] Yield was calculated using UV-Vis from the measured absorbance values at 284 nm and the molar extinction coefficient. [b] Yield was measured by HPLC using 0.05% H_2SO_4–water as a mobile phase.

pattern shown in Fig. 1(e) suggested the diffraction spots for anatase TiO_2. Further evidence in support of the TiO_2 samples being composed of uniform tiny spherical nanoparticles came from the FE-SEM images (Fig. 1(f)).

HR-TEM images of TiO_2 nanoparticles calcined at 500 °C (Fig. 2(a) and 2(b)) were taken for determining detail crystalline information such as lattice fringes and interface information. Lattice fringes are quite clear in both HR-TEM images. Fig. 2(a) shows only (101) plane, while planes (101) and (004) are observed in Fig. 2(b). Distance between (101) plane is calculated to be 0.35 nm and that of (004) plane is 0.238 nm. These results from the HR-TEM analysis agrees well with the wide-angle XRD of the anatase TiO_2 materials.

The N_2 adsorption/desorption isotherms of aspartic acid templated TiO_2 sample (Fig. 3(a)) can be classified as type IV corresponding to the mesoporous materials.[22] Further, hysteresis loop of type H3, indicating substantial textural mesoporosity is also observed. BET surface area and pore volume of this sample was 51.5 m^2g^{-1} and 0.14 ccg^{-1}. The pore size distribution of the sample employing the Non Local Density Functional Theory (NLDFT) method suggested a peak pore width of 9.5 nm (Fig. 3 (b)). The pore width obtained from powder XRD and HR-TEM analysis agrees well with this data obtained from N_2 sorption analysis.

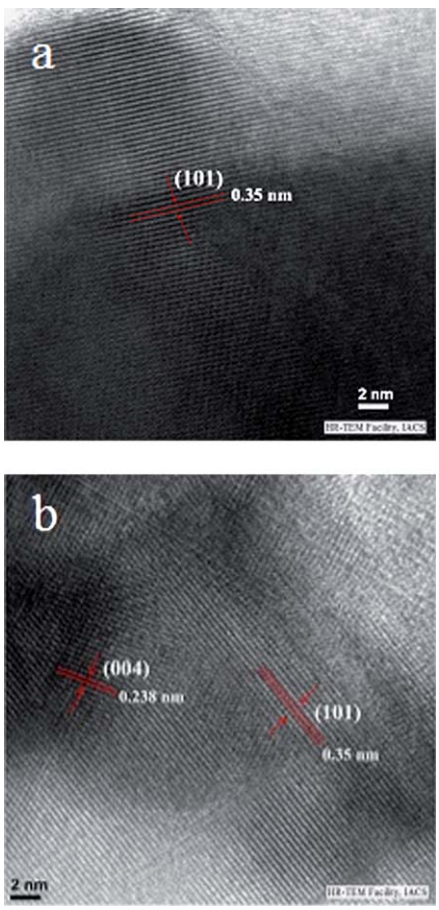

Fig. 2 HR-TEM images of TiO_2 sample calcined at 500 °C; **a**: showing (101) plane **b**: showing (101) and (004) planes.

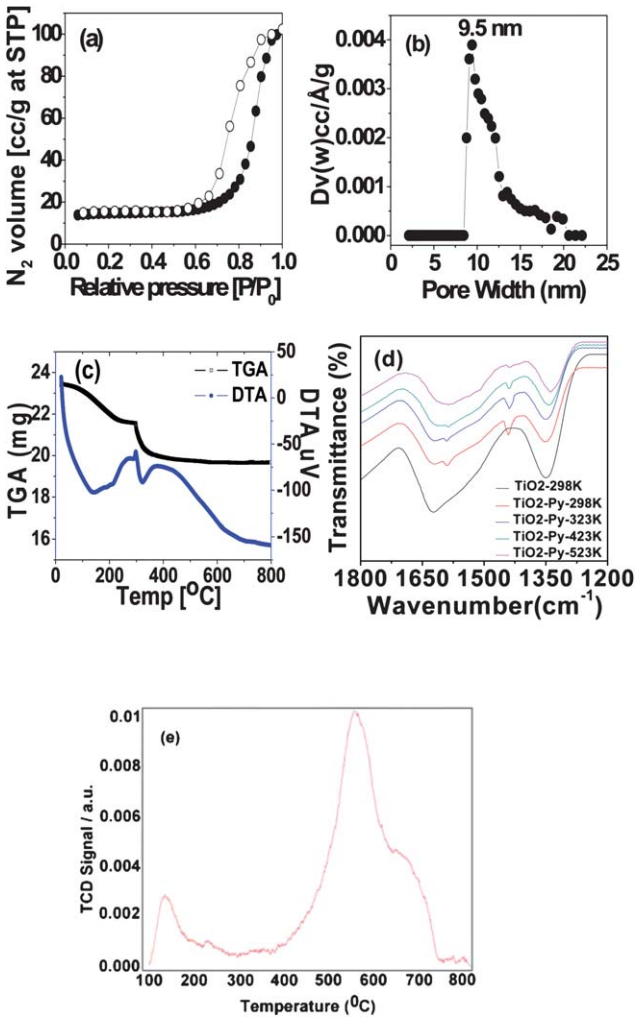

Fig. 3 **a**: N_2 adsorption (●)-desorption (○) isotherms of the calcined TiO_2 at 77 K. **b**: The respective pore size distribution using NLDFT method are shown. **c**: TG/DTA curves for the prepared TiO_2 sample; **d**: FT IR spectra of mesoporous TiO_2 sample (298 K) and pyridine desorbed TiO_2 sample at (298 K, 323 K, 423 K, and 523 K); **e**: Temperature programmed desorption (TPD) of ammonia over mesoporous TiO_2 nanoparticles.

The TG/DTA curves (Fig. 3(c)) show two weight loss stages, and the relevant DTA peaks are close to 142 °C and 323 °C. The first weight loss is caused by the evaporation of physically adsorbed water and the second weight loss, along with the exothermic nature in the DTA curve, suggests a peptide combustion and the temperature was high enough to burn off the peptide bonded to the metal (Fig. 3(c)). FTIR spectra of the pyridine adsorbed mesoporous TiO_2 nanoparticles shows two characteristic bands at 1589 and 1440 cm^{-1} (Fig. 3(d)). The band at 1440 cm^{-1} could be attributed to the adsorbed pyridine at the Lewis acid site[38] and with increase in desorption temperature this band showed slow decrease in intensity. This result suggested the presence of considerably strong Lewis acid site in our self-assembled mesoporous TiO_2 nanoparticles. Further, NH_3-TPD results (Fig. 3(e)) showed very high desorption temperature (400–750 °C) with peaks at *ca.* 560 and 652 °C). Total acidity of the mesoporous TiO_2 amounts to 0.27 mmol g^{-1}. Strong Lewis

acidity together with textural mesoporosity could be exploited in acid catalyzed reactions over these self-assembled TiO_2 nanoparticles.

Several heterogeneous catalysts containing acidic sites are known to catalyze the dehydration of carbohydrates to HMF in organic solvents,[39,40] ionic liquids,[31,32] and biphasic organic-ionic liquid medium.[41,42] To the best of our knowledge, mesoporous TiO_2 nanoparticulate material with Lewis acidic sites is yet to be explored for the conversion of carbohydrates to HMF in ionic liquid solvents. With this aim, catalytic effectiveness of the mesoporous TiO_2 nanoparticles was investigated for the conversion of fructose and glucose into HMF at varying reaction conditions. As shown in Table 1, fructose dehydration reaction with 50 mg mesoporous TiO_2 catalyst produced 31.5% HMF under microwave irradiation for 2 min in aqueous medium at 120 °C. Upon continuing the same reaction for 5 min, only 3% increase in HMF yield was noted. In DMSO, the yield of HMF improved to 49.5% under microwave irradiation for 2 min at 130 °C. Under comparable reaction conditions, only 23.6% HMF yield was recorded without TiO_2 catalyst (Table 1, entry 3). It might be due to the catalytic activity of the solvent DMSO which was reported to assist the dehydration of fructose at high temperature (140 °C) to form HMF under microwave-assisted heating.[43] Nevertheless, a comparison of HMF yields from fructose dehydration reactions with and without Lewis acidic TiO_2 catalyst (49.5% with catalyst; 23.6% without catalyst) confirmed the effectiveness of the catalyst.

Ionic liquid solvents are known to have beneficial effect in improving HMF yield obtained from the catalytic dehydration of carbohydrates.[31,32] However, ionic liquid is expensive. Therefore in the present study, *N*,*N*-dimethylacetamide (DMA)-LiCl solvent was utilized to examine the effect of TiO_2 catalyst on HMF yield. DMA-LiCl solvent is known to form $DMA \cdot Li^+$ macrocations, resulting in highly ion-paired chloride ions.[44] When fructose dehydration reaction was carried out in DMA-LiCl (10 wt%) solvent at 130 °C for 2 min, a significant improvement in HMF yield (61.0%) was noted even without the added catalyst in comparison with 23.6% HMF yield in DMSO under similar conditions. The yield of HMF further improved to 74.8% when DMA-LiCl solvent mediated fructose dehydration was repeated with the mesoporous TiO_2 catalyst. A further improvement in HMF yield to 82.3% was observed when DMA-LiCl solvent mediated fructose dehydration with the mesoporous TiO_2 catalyst was repeated in the presence of 20 wt% 1-butyl-3-methylimidazolium chloride ([BMIM]Cl) as an additive. The beneficial effect of [BMIM]Cl additive might be due to the formation of a higher concentration of weakly ion-paired chloride ions.

Glucose is a potential substrate for HMF synthesis due to its higher abundance.[45] It is reported that only 7% HMF yield was obtained from the glucose dehydration reaction with the metal oxide (TiO_2, ZrO_2) catalyst at 200 °C in HCW.[34] In the present study, the performance of mesoporous TiO_2 catalyst for glucose dehydration reaction was tested in water, DMSO and DMA-LiCl solvents by carrying out the reactions with and without catalyst in each solvent and comparing the results. Entries 8 and 9 in Table 1 showed the formation of 0% and 13.4% HMF from glucose dehydration with and without TiO_2 catalyst in water. Similarly, a comparison of entries 11 and 12 in Table 1 revealed glucose dehydration with the TiO_2 catalyst produced 14.4% more HMF than without catalyst in DMSO. A comparison of entries 13, 14 and 15 in Table 1 suggested the HMF yields obtained from the glucose dehydration in DMA-LiCl and DMA-LiCl/([BMIM]Cl solvents with the mesoporous TiO_2 catalyst were 17.4% and 26.1% more than that obtained without catalyst. These experiments with and without catalysts in different solvents further proved that the mesoporous TiO_2 nanomaterial is an active catalyst for the dehydration of glucose and fructose, and that the presence of considerable surface acidity of the mesoporous TiO_2 is responsible for the catalytic activity. In the presence of [BMIM]Cl additive, mesoporous TiO_2 catalyzed dehydration of fructose and glucose produced maximum 82.3% and 30.2% HMF, respectively. It is worth to note that the yield of HMF from glucose substrate is significantly lower than that from fructose in all solvents. The lower HMF yields from glucose can be explained by the involvement of additional sequential steps in its dehydration process, namely, mutarotation and isomerization of glucose into fructose followed by dehydration of fructose to HMF.[46,47]

Table 2 Results of recyclability study of TiO_2 catalyst in DMA-LiCl for the dehydration of fructose under microwave assisted heating at 140 °C[a]

Cycle no.	Fructose (mg)	*t* (min)	*T*/°C	HMF yield
1	100	2	130	74.8
2	100	2	130	73.8
3	100	2	130	73.0
4	100	2	130	71.2
5	100	2	130	69.5

[a] Solvent = DMA-LiCl, TiO_2 NP = 50 mg.

The reusability of the mesoporous TiO_2 catalyst was examined for fructose dehydration reaction in DMA-LiCl by recycling the spent catalyst. Prior to recycle the catalyst for the next run, the reaction mixture was filtered and HMF component was extracted from the reaction mixture with diethyl ether. The solid TiO_2 catalyst was recovered by filtration, washed with distilled water and dried. The catalyst was reused for five catalytic cycles without significant loss in HMF yields (Table 2).

Conclusions

In conclusion, self-assembled mesoporous TiO_2 nanoparticulate material was synthesized at room temperature by precipitation method from titanium isopropoxide and DL-aspartic acid as a template. Amino acid templating pathway provided uniform size and shape-controlled TiO_2 nanoparticle with considerably high surface area as revealed from the N_2 sorption studies. Pyridine-IR and NH_3-TPD studies confirmed the presence of considerable Lewis acidic sites in the mesoporous TiO_2 material. The effective catalytic activity of TiO_2 nanoparticles for the microwave-assisted conversion of fructose and glucose into HMF was investigated in aqueous, organic and DMA-LiCl solvent. Using imidazolium ionic liquid as an additive, mesoporous TiO_2 catalyzed dehydration of fructose and glucose produced maximum 82.3% and 30.2% HMF in DMA-LiCl, respectively. The spent TiO_2 catalyst was recycled for five catalytic cycles without significant loss in HMF yield.

Acknowledgements

The authors gratefully acknowledge financial support by the University Grant Commission (UGC), India and the University of Delhi. SD thanks UGC, India for a DS Kothari Postdoctoral Research Fellowship.

Notes and references

1 J. J. Wu, X. J. Lu, L. L. Zhang, F. Q. Huang and F. F. Xu, *Eur. J. Inorg. Chem.*, 2009, 2789–2795.
2 S. C. Yang, D. J. Yang, J. Kim, J. M. Hong, H. G. Kim, I. D. Kim and H. Lee, *Adv. Mater.*, 2008, **20**, 1059–1064.
3 X. J. Lu, X. L. Mou, J. J. Wu, D. W. Zhang, L. L. Zhang, F. Huang, F. F. Xu and S. M. Huang, *Adv. Funct. Mater.*, 2010, **20**, 509–515.
4 M. Luo, K. Cheng, W. J. Weng, C. L. Song, P. Y. Du, G. Shen and G. R. Han, *Nanoscale Res. Lett.*, 2009, **4**, 809–813.
5 J. P. Wang, Y. Bai, M. Y. Wu, J. Yin and W. F. Zhang, *J. Power Sources*, 2009, **191**, 614–618.
6 H. X. Li, Z. F. Bian, J. Zhu, D. Q. Die, G. S. Li, Y. N. Huo, H. Li and Y. F. Lu, *J. Am. Chem. Soc.*, 2007, **129**, 8406–8407.
7 S.-H. A. Lee, N. M. Abrams, P. G. Hoertz, G. D. Barber, L. I. Halaoui and T. E. Mallouk, *J. Phys. Chem. B*, 2008, **112**, 14415–14421.
8 U. Jeong, S. H. Im, P. H. C. Camargo, J. H. Kim and Y. Xia, *Langmuir*, 2007, **23**, 10968–10975.
9 S. K. Das, M. K. Bhunia and A. Bhaumik, *Dalton Trans.*, 2010, **39**, 4382–4390.
10 M. R. Hoffmann, S. T. Martin, W. Y. Choi and D. W. Bahnemann, *Chem. Rev.*, 1995, **95**, 69–96.
11 M. Epifani, R. Diaz, J. Arbiol, E. Comini, N. Sergent, T. Pagnier, P. Siciliano, G. Taglia and J. R. Morante, *Adv. Funct. Mater.*, 2006, **16**, 1488–1498.
12 E. V. Skorb, D. G. Shchukin, H. Moehwald and D. V. Sviridov, *J. Mater. Chem.*, 2009, **19**, 4931–4937.
13 Z. Y. Liu, X. T. Zhang, S. Nishimoto, T. Murakami and A. Fujishima, *Environ. Sci. Technol.*, 2008, **42**, 8547–8551.
14 P. Hartmann, D. K. Lee, B. M. Smarsly and J. Janek, *ACS Nano*, 2010, **4**, 3147–3154.
15 M. C. Long, R. Beranek, W. M. Cai and H. Kisch, *Electrochim. Acta*, 2008, **53**, 4621–4626.
16 N. Pal, M. Paul, A. Bera, D. Basak and A. Bhaumik, *Anal. Chim. Acta*, 2010, **674**, 96–101.
17 C. T. Kresge, M. E. Leonowicz, W. J. Roth, J. C. Vartuli and J. S. Beck, *Nature*, 1992, **359**, 710–712.
18 Y. Goto and S. Inagaki, *Chem. Commun.*, 2002, 2410–2411.
19 V. Meynen, P. Cool and E. F. Vansant, *Microporous Mesoporous Mater.*, 2009, **125**, 170–223.
20 A. Mitra, A. Bhaumik and T. Imae, *J. Nanosci. Nanotechnol.*, 2004, **4**, 1052–1055.
21 J. Liu, F. Liu, K. Gao, J. S. Wu and D. F. Xue, *J. Mater. Chem.*, 2009, **19**, 6073–6084.
22 A. P. Patra, S. K. Das and A. Bhaumik, *J. Mater. Chem.*, 2011, **21**, 3925–3930.
23 P. Xu, T. Xu, J. Lu, S. Gao, N. S. Hosmane, B. Huang, Y. Dai and Y. Wang, *Energy Environ. Sci.*, 2010, **3**, 1128–1134.
24 Z. Zheng, B. Huang, X. Qin, X. Zhang and Y. Dai, *Chem.–Eur. J.*, 2010, **16**, 11266–11270.
25 S. Ding, F. Huang, X. Mou, J. Wu and X. Lu, *J. Mater. Chem.*, 2011, **21**, 4888–4892.
26 R. Inaba, T. Fukahori, M. Hamamoto and T. Ohno, *J. Mol. Catal. A: Chem.*, 2006, **260**, 247–254.
27 Y. D. Wang, A. N. Zhou and Z. Y. Yang, *Mater. Lett.*, 2008, **62**, 1930–1932.
28 Z. Zhang, F. Zuo and P. Feng, *J. Mater. Chem.*, 2010, **20**, 2206–2212.
29 T. A. Werpy, G. Petersen, *Top value added chemicals from biomass*, U. S. Department of Energy (DOE), Golden, CO, DOE/GO-102004-1992, 2004.
30 F. W. Lichtenthaler, *Acc. Chem. Res.*, 2002, **35**, 728–737.
31 M. E. Zakrzewska, E. Bogel-Lukasik and R. Bogen-Lukasik, *Chem. Rev.*, 2011, **111**, 397–417.
32 T. Stålberg, W. Fu, J. M. Woodley and A. Riisager, *ChemSusChem*, 2011, **4**, 451–458.
33 M. J. Climent, A. Corma and S. Iborra, *Green Chem.*, 2011, **13**, 520–540 and references therein.
34 X. Qi, M. Watanabe, T. M. Aida and R. L. Smith, Jr., *Catal. Commun.*, 2008, **9**, 2244–2249.
35 M. Watanabe, Y. Aizawa, T. Lida, R. Nishimura and H. Inomata, *Appl. Catal., A*, 2005, **295**, 150–156.
36 A. Chareonlimkun, V. Champreda, A. Shortipruk and N. Laosiripojana, *Bioresour. Technol.*, 2010, **101**, 4179–4186.
37 M. Paul, N. Pal, P. R. Rajamohanan, B. S. Rana, A. K. Sinha and A. Bhaumik, *Phys. Chem. Chem. Phys.*, 2010, **12**, 9389–9394.
38 H. Yan, Y. Yang, D. Tong, X. Xiang and C. Hu, *Catal. Commun.*, 2009, **10**, 1558–1563.
39 P. Vinke and H. Vanbekkum, *Starch/Stärke*, 1992, **44**, 90–96.
40 G. A. Halliday, R. J. Young and V. V. Grushin, *Org. Lett.*, 2003, **5**, 2003–2005.
41 X. H. Qi, M. Watanabe, T. M. Aida and R. L. Smith, *Green Chem.*, 2009, **11**, 1327–1331.
42 X. H. Qi, M. Watanabe, T. M. Aida and R. L. Smith, *ChemSusChem*, 2009, **2**, 944–946.
43 A. S. Amarasekara, L. D. Williams and C. C. Ebede, *Carbohydr. Res.*, 2008, **343**, 3021–3024.
44 J. B. Binder and R. T. Raines, *J. Am. Chem. Soc.*, 2009, **131**, 1979–1985.
45 A. Corma, S. Iborra and A. Velty, *Chem. Rev.*, 2007, **107**, 2411–2502.
46 H. Zhao, J. E. Holladay, H. Brown and Z. C. Zhang, *Science*, 2007, **316**, 1597–1520.
47 S. De, S. Dutta and B. Saha, *Green Chem.*, 2011, DOI: 10.1039/c1gc15550d.

